Diastereoselective Arbuzov dealkylation and evidence for phosphorus-carbon bond activation of prochiral cobalt(III) phosphonite complexes

Brian J. Boone, Chet R. Jablonski, Peter G. Jones, Michael J. Newlands, and Yongfei Yu

Organometallics, **1993**, 12 (8), 3042-3050• DOI: 10.1021/om00032a029 • Publication Date (Web): 01 May 2002

Diastereoselective Arbuzov Dealkylation and Evidence for Phosphorus–Carbon Bond Activation of Prochiral Cobalt(III) Phosphonite Complexes

Brian J. Boone, Chet R. Jablonski,* Peter G. Jones,[1] Michael J. Newlands, and Yongfei Yu

Department of Chemistry, Memorial University, St. John's, Newfoundland, Canada A1B 3X7

Received March 16, 1993

(S_c)-(η^5-Cp)CoI_2(PPh_2NHC*H(Me)Ph) reacts with 1 equiv of dimethyl *tert*-butyl- or ethylphosphonite in methylene chloride solution to give diastereomeric P-chiral phosphinate Arbuzov products (R,S_{Co};R,S_P;S_C)-(η^5-Cp)CoI(PPh_2NHC*H(Me)Ph)(P(O)(OMe)(*t*-Bu)) (**3a**) and (R,S_{Co};R,S_P;S_C)-(η^5-Cp)CoI(PPh_2NHC*H(Me)Ph)(P(O)(OMe)(Et)) (**3b**), respectively. Apparent phosphorus–carbon bond cleavage also occurs to give (R,S_{Co};S_C)-(η^5-Cp)CoI(PPh_2NHC*H(Me)-Ph)(P(O)$(OMe)_2$) (**4**), which was isolated in low yield after aerial workup. Two diastereomers of the *tert*-butyl series **3a** and one diastereomer of the four isolated for the ethyl series **3b** were characterized by single-crystal X-ray diffraction. (S_{Co};R_P;S_C)-**3a-1** crystallizes in the space group $P2_12_12_1$ with a = 9.815(4) Å, b = 14.314(6) Å, c = 21.120(9) Å, V = 2967(2) Å^3, Z = 4, and R_F = 2.83% for 5958 reflections ($F > 4.0\sigma(F)$) at 198 K. (R_{Co};S_P;S_C)-**3a-2** crystallizes in the space group $P2_1$ with a = 13.073(5) Å, b = 8.731(2) Å, c = 13.537(5) Å, β = 106.49(3)°, V = 1481.5(9) Å^3, Z = 2, and R_F = 3.19% for 4846 reflections ($F > 4.0\sigma(F)$) at 198 K. (R_{Co};S_P;S_C)-**3b-2** crystallizes in the space group $P2_12_12_1$ with a = 8.7004(7) Å, b = 12.0769(18) Å, c = 27.490(3) Å, V = 2888.5(6) Å^3, Z = 4, and R_F = 4.4% for 3118 reflections ($F > 2.5\sigma(F)$) at 297 K. The absolute configurations of all diastereomers were assigned on the basis of crystallographic results, circular dichroism, and chemical cycles involving Co epimerization. P═O···H—N intramolecular hydrogen bonding establishes a "*chaise* longue" conformation with pseudoaxial η^5-Cp and pseudoequatorial iodide in the solid state. Proton nuclear Overhauser difference (NOED) spectra show that the solid-state conformation is retained in solution. Optical yields increased with increasing steric demands of the prochiral phosphonite substituent. A model based on 1,3-diaxial steric interactions in the transition state leading to dealkylation is proposed to account for the observed Co→P chiral induction.

Introduction

Previous work in this laboratory[2,3] showed that the substitution of prochiral iodide in the pseudooctahedral aminophosphine η^5-Cp cobalt(III) complex 1 with 1 equiv of PR$(OMe)_2$ affords the chiral phosphonite complex (R,S_{Co})-**2c** that subsequently dealkylates via an Arbuzov-like rearrangement[4–26] to give P-chiral phosphinate products as a diastereomeric mixture, (R,S_{Co};R,S_P;S_C)-**3c**. Diastereomeric excesses of up to 80% in the case of PhP$(OMe)_2$[2] demonstrated strong Co→P chiral induction in the dealkylation step.

Analysis of the observed optical inductions was based on a transition-state model requiring intramolecular P═O···H—N hydrogen bonding between the basic phosphoryl oxygen and the aminophosphine NH which formed a "*chaise longue*" conformation. Strong 1,3-diaxial steric interactions between phenyl groups on the aminophosphine and phosphonite were proposed to favor the transition state leading to the R_{Co};S_P product (cf. Chart I). Since the model suggested a direct steric involvement of the phosphonite substituents, we sought a more comprehensive demonstration of Co→P chiral introduction in the key Arbuzov dealkylation step. This work reports an extension of our earlier results[2] to structural

(1) Current address: Institut für Anorganische und Analytische Chemie, Technische Universitat, 3000 Braunschweig, Germany.

(2) Brunner, H.; Jablonski, C. R.; Jones, P. G. *Organometallics* 1988, *7*, 1283–1292.
(3) Jablonski, C. R.; Ma, H.; Chen, Z.; Hynes, R. C.; Bridson, J. N.; Bubenik, M. P. *Organometallics* 1993, *12*, 917–926.
(4) Pidcock, A.; Waterhouse, C. R. *J. Chem. Soc. A* 1970, 2080–2086.
(5) Brunner, H.; Riepl, G.; Benn, R.; Rufinska, A. *J. Organomet. Chem.* 1983, *253*, 93–115.
(6) Haines, R. J.; Du Preez, A. L.; Marais, I. L. *J. Organomet. Chem.* 1971, *28*, 405–413.
(7) Werner, H.; Harder, V. *Helv. Chim. Acta* 1973, *56*, 1620–1629.
(8) Clemens, J.; Neukomm, H. W. *Helv. Chim. Acta* 1974, *57*, 2000–2010.
(9) King, R. B.; Reiman, R. H. *Inorg. Chem.* 1976, *15*, 179–183.
(10) Werner, H.; Juthani, B. *J. Organomet. Chem.* 1981, *209*, 211–218.
(11) Day, V. W.; Tavanaiepour, I.; Abdel-Meguid, S. S.; Kirner, J. F.; Goh, L.-Y. *Inorg. Chem.* 1982, *21*, 657–663.
(12) Brill, T. B.; Landon, S. J. *J. Am. Chem. Soc.* 1982, *104*, 6571–6575.
(13) Brill, T. B.; Landon, S. J. *Inorg. Chem.* 1984, *23*, 1266–1271.
(14) Brill, T. B.; Landon, S. J. *Chem. Rev.* 1984, *84*, 577–585.
(15) Sullivan, R. J.; Bao, Q. B.; Landon, S. J.; Rheingold, A. L.; Brill, T. B. *Inorg. Chim. Acta* 1986, *111*, 19–24.
(16) Bao, Q. B.; Brill, T. B. *Organometallics* 1987, *6*, 2588–2589.
(17) Schleman, E. V.; Brill, T. B. *J. Organomet. Chem.* 1987, *323*, 103–109.
(18) Gibson, D. H.; Ong, T.-S.; Ye, M.; Franco, J. O.; Owens, K. *Organometallics* 1988, *7*, 2569–2570.
(19) Jablonski, C. R.; Burrow, T.; Jones, P. G. *J. Organomet. Chem.* 1989, *370*, 173–185.
(20) Bruggeller, P.; Hubner, T.; Gieren, A. *Z. Naturforsch., B* 1989, *44B*, 800–805.
(21) Nakazawa, H.; Morimasa, K.; Kushi, Y.; Yoneda, H. *Organometallics* 1988, *7*, 458–463.
(22) Nakazawa, H.; Yasunori, K.; Katsuhiko, M. *Organometallics* 1989, *8*, 2851–2856.
(23) Nakazawa, H.; Yamaguchi, M.; Kubo, K.; Miyoshi, K. *J. Organomet. Chem.* 1992, *428*, 145–153.
(24) Nakazawa, H.; Kadoi, Y.; Itoh, T.; Mizuta, T.; Miyoshi, K. *Organometallics* 1991, *10*, 766–770.
(25) Ji, H.-L.; Nelson, J. H.; De Cian, A.; Fischer, J. *Organometallics* 1992, *11*, 1618–1626.
(26) Jablonski, C. R.; Ma, H.; Hynes, R. C. *Organometallics* 1992, *11*, 2796–2802.

0276-7333/93/2312-3042$04.00/0

Table I. Physical and IR Data

compd	anal. found (calc)			mp (°C)	$[\alpha]_{436}$ (deg)	abs confign	% de	$\nu_{P=O}$, δ_{P-OC}, δ_{PO-C} (cm^{-1})
	% C	% H	% N					
3a-1	52.27 (52.12)	5.47 (5.39)	1.59 (2.03)	140.8–141.5	+1724	$S_{Co};R_P;S_C$[a]	100[c]	1102 (s), 1029 (s), 698 (s)
3a-2				89–93	−2615	$R_{Co};S_P;S_C$[a]	100[d]	1111 (s), 1026 (s), 696 (s)
3b-1						$S_{Co};R_P;S_C$[b]	≤25[c]	1124 (s), 1020 (s), 698 (s)
3b-2	50.53 (50.70)	5.03 (5.01)	1.63 (2.11)	158.0–159.5		$R_{Co};S_P;S_C$[a]	≤14[d]	1124 (s), 1019 (s), 697 (s)
3b-3						$S_{Co};S_P;S_C$[b]		
3b-4						$R_{Co};R_P;S_C$[b]		

[a] Determined crystallographically. [b] Determined from chiroptical data and epimerization studies. [c] $S_{Co};R_P;S_C/S_{Co};S_P;S_C$. [d] $R_{Co};S_P;S_C/R_{Co};R_P;S_C$.

Scheme I

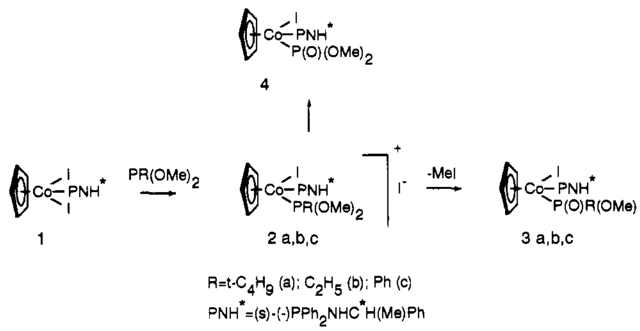

Chart I

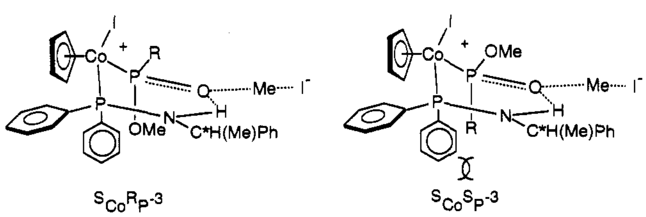

analogs wherein the phosphonite R group varies from ethyl to *tert*-butyl.

Results and Discussion

Reaction of (η^5-Cp)CoI$_2$(PPh$_2$NHC*H(Me)Ph) with *t*-BuP(OMe)$_2$ and EtP(OMe)$_2$. Reaction of 1 equiv of dimethyl *tert*-butylphosphonite with the aminophosphine-substituted halide complex 1 in methylene chloride leads to a complex reaction mixture from which several products were isolated in low yield. Preparative thick-layer radial chromatography separated starting material and four products. These were identified (*vide infra*), in order of decreasing TLC R_f values, as two of the four possible diastereomeric Arbuzov dealkylation products **3a-1** and **3a-2**, and both diastereomers of the previously reported[2] dimethyl phosphonate **4-1** and **4-2**. Further purification was accomplished by recrystallization from hexane/toluene at 243 K. Although it had been erroneously reported[27] that alkyl *tert*-butylphosphonites do not undergo Arbuzov rearrangement, NMR experiments show that reaction with methyl iodide and subsequent dealkylation is very fast and in fact limits the yield of organometallic products of Scheme I. Addition of 1 equiv of MeI to a CD_2Cl_2 solution of *t*-BuP(OMe)$_2$ in an NMR tube showed rapid, quantitative conversion to *t*-BuP(O)(Me)(OMe) (δ 3.66 (d, J = 10.3 Hz, 3H)), OMe; δ 1.34 (d, J = 12.5 Hz, 3H), PMe; δ 1.12 (d, J = 15.4 Hz, 9H), PCMe$_3$). ^{1}H NMR experiments which monitored the progress of the reaction of 1 with *t*-BuP(OMe)$_2$ to determine the kinetic product distribution detected **3a-1** and **3a-2** in a ca. 1:1 ratio. These experiments did not conclusively demonstrate the absence of other diastereomers, since the Cp and OMe regions were complex.

Heating methylene chloride solutions of 1 with dimethyl ethylphosphonite in a sealed tube at 333 K resulted in a slow color change from dark purple to yellow-brown. Preparative thick-layer radial chromatography of the complex crude reaction mixture gave incomplete separation of four low-yield, diastereomer, yellow-green methyl ethylphosphinate products, **3b-1**, **3b-2**, **3b-3**, and **3b-4** (in order of decreasing TLC R_f values). Dimethylphosphonate products **4-1** and **4-2** were also identified in low-R_f fractions collected. The methyl ethylphosphinate products were found to be stereochemically labile in solution; however, attempts to determine the kinetic product distribution by ^{1}H NMR were unsuccessful. TLC analysis showed that isomerization in solution *specifically* interconverts **3b-1** ↔ **3b-4** and **3b-2** ↔ **3b-3**. Since a related series in which the substitution-labile iodide is replaced by a corresponding perfluoro group is configurationally stable even on heating in solution for several weeks at 333 K,[26] we presume that diastereomer interconversion proceeds via Co epimerization[2,26] as a result of homolytic Co–I bond cleavage and that the P-chiral center is stereochemically robust.

Characterization of the Phosphinate and Phosphonate Products. Complexes **3a-1**, **3a-2**, and **3b-2** were fully characterized by elemental analysis, IR, ^{1}H and ^{13}C NMR, and X-ray crystallographic studies. The structures of the remaining **3b** diastereomers were established spectroscopically. Infrared spectra showed strong $\nu_{P=O}$, δ_{P-OC}, and δ_{PO-C} modes in the ranges 1102–1124, 1019–1038, and 697–699 cm^{-1}, respectively, for all phosphinate complexes. All diastereomers displayed distinct ^{1}H and ^{13}C NMR chemical shifts (cf. Tables II and III), and this was particularly evident for the C**Me* doublet and the C**H* multiplet of the aminophosphine ligand[28] (cf. Table II). The presence of chiral Co, P, and C atoms results in diastereotopic P*Ph*$_2$ and P—CH_AH_B– groups, which are reflected in the NMR spectra of the complexes **3**. ^{1}H NMR parameters for the P—CH_AH_B—C group of **3b** were extracted from the observed second-order ABM$_3$X spin system by computer simulation. In general, pairs of PPh$_2$ *ipso*, *ortho*, *meta*, and *para* ^{13}C resonances were observed (cf. Table III). Diastereotopic ^{1}H chemical shift differences of H_A and H_B for the ethyl derivatives **3b** are quite large, typically in the range of 0.5–1.0 ppm (cf. Table II). Consistent with the presence of a strong, intramolecular N—H···P=O hydrogen bond, the chemical shift of the

(27) Crofts, P. C.; Parker, D. M. *J. Chem. Soc. C* **1970**, 2342.

(28) Brunner, H. *Adv. Organomet. Chem.* **1980**, *18*, 151–206.

Table II. ^{1}H NMR Data[a]

compd	Ph	NH[b]	Cp	OMe	C*H[c]	C*Me	R
3a-1	7.86 (m), 7.71 (m), 7.34 (m), 7.18 (m), 6.93 (m), 6.78 (m)	6.11 (6.7, 7.7)	4.92 (s)	3.05 (d, 9.3)	3.68 (6.7, 9.7, 6.7)	1.31 (6.7, 1.2)[d]	1.40 (d, 15.5)
3a-2	7.94 (m), 7.81 (m), 7.51 (m), 7.21 (m), 7.08 (m), 6.96 (m)	5.76 (6.7, 11.0)	4.90 (s)	3.23 (d, 9.2)	3.89 (6.7, 10.8, 6.7)	1.34 (d, 6.7)	1.42 (d, 15.5)
3b-1	7.99 (m), 7.51 (m), 7.39 (m), 7.22 (m), 6.96 (m)	6.45 (7.0, 11.0)	4.82 (s)	3.51 (d, 9.9)	3.65 (7.0, 9.5, 7.0)	1.29 (7.0, 0.9)[d]	1.32 (7.7, 7.7, 16.7),[e] 3.10 (7.7, 5.5, 14.5),[f] 2.64 (7.5, 4.8, 14.6)[f]
3b-2	7.93 (m), 7.75 (m), 7.50 (m), 7.20 (m), 7.13 (m)	6.24 (6.9, 13.5)	4.80 (s)	3.37 (d, 9.8)	3.93 (6.9, 10.6, 6.9)	1.32 (m)	1.32 (m), 3.13 (7.7, 5.7, 14.6),[f] 2.66 (7.7, 4.6, 14.6)[f]
3b-3	8.07 (m), 7.47 (m), 7.33 (m), 7.04 (m), 6.96 (m)	5.75 (6.6, 11.0)	4.86 (s)	3.81 (d, 9.8)	3.64 (6.6, 9.6, 6.6)	1.23 (6.6, 0.9)[d]	1.05 (m), 1.78 (m), 0.88 (m)
3b-4	7.95 (m), 7.69 (m), 7.53 (m), 7.18 (m), 7.08 (m), 6.90 (m)	5.63 (6.9, 14.8)	4.83 (s)	3.77 (d, 9.7)	3.96 (6.9, 9.5, 6.9)	1.40 (d, 6.9)	1.07 (7.5, 7.5, 15.9),[e] 1.86 (7.5, 5.1, 14.5),[f] 1.27 (m)

[a] Conditions and definitions: measured at 300.1 MHz; chemical shifts ($CDCl_3$) in ppm relative to internal TMS; m = multiplet; s = singlet; d = doublet; J values (given in parentheses) in Hz. [b] dd ($^3J_{HH}$, $^2J_{PH}$). [c] m ($^3J_{HH}$, $^3J_{PH}$, $^3J_{HMe}$). [d] Doublet of doublets ($^3J_{HH'}$, $^4J_{PH}$). [e] Doublet of triplets ($^3J_{HH'_a}$, $^3J_{HH'_b}$, $^3J_{PH}$). [f] Overlapping quartet of quartets ($^3J_{HMe}$, $^2J_{PH}$, $^2J_{HH}$).

Table III. ^{13}C NMR Spectra[a]

compd	C—C_6H_5	P—C_6H_5	Cp	OMe	C*	C**Me*	P(O)*C*C	P(O)C*C*
3a-1	*i*: 147.71 *o*/*m*: 126.08 *p*: 125.56	*i*: 133.0 (d, 60.0) *o*/*m*: 135.40 (d, 8.8), 131.96 (d, 10.2) *p*: 131.02 (s), 129.47 (s)	83.38	51.52 (d, 8.5)	54.90 (d, 5.6)	26.45 (d, 10.2)	nf[b]	28.54
3a-2	*i*: 146.20 *o*/*m*: 127.34, 125.91 *p*: 125.52	*i*: 137.45 (d, 39.9), 134.00 (d, 60.0) *o*/*m*: 134.05 (d, 9.7), 132.29 (d, 9.6), 128.11 (d, 9.0), 127.45 (d, 11.5) *p*: 130.63, 129.97	88.38	51.59 (d, 8.7)	53.68 (d, 11.1)	27.40	29.70	28.97
3b-1	*i*: 146.83 *o*/*m*: 127.50, 125.91 *p*: 125.53	*i*: 138.13 (d, 49.7), 132.99 (d, 56.3) *o*/*m*: 134.36 (d, 9.4), 131.47 (d, 9.9), 127.59 (d, 13.6), 127.25 (d, 9.5) *p*: 133.86, 132.61	88.45	51.69 (d, 8.9)	54.19 (d, 8.8)	26.49 (d, 8.2)	41.90 (d, 40.8)	9.52 (d, 6.6)
3b-2	*i*: 146.25 *o*/*m*: 127.21, 125.55 *p*: 125.35	*i*: 137.20 (d, 44.5), 133.22 (d, 60.8) *o*/*m*: 133.87 (d, 9.4), 131.64 (d, 9.4), 127.86 (d, 9.4), 127.21 (d, –) *p*: 130.30, 129.91	89.10	52.31 (d, 9.0)	53.80 (d, 10.3)	27.11 (d, 3.8)	41.70 (dd, 40.8, 4.4)	9.30 (d, 6.8)
3b-4	*i*: 145.89 *o*/*m*: 128.47, 125.86 *p*: 125.43	*i*: 136.66 (d, 45.6), 133.23 (d, 57.4) *o*/*m*: 133.84 (d, 10.6), 132.36 (d, 9.3), 128.40 (d, 11.0), 127.12 (d, 13.6) *p*: 130.68, 130.32	88.63	53.72 (d, 10.30)	54.21 (d, 7.3)	27.36 (d, 4.8)	35.63 (d, 39.9)	7.94 (d, 8.2)

[a] Conditions: Measured at 75.47 MHz; $CDCl_3$ solvent; chemical shifts in δ relative to solvent peak at 77.0 ppm; coupling constants (given in parentheses) in Hz. [b] nf = not found.

N—H proton of **3** is relatively concentration independent and strongly deshielded (cf. Table II) compared to that of **1**.[29]

^{1}H NMR analysis established that the low-yield, lowest R_f products **4-1** and **4-2**, isolated from the reaction of *tert*-butylphosphonite with **1**, were identical with the dimethyl phosphonate complexes CpCoI(PPh_2NHC*H(Me)Ph)-(P(O)($OMe)_2$) reported previously from the reaction of **1** with trimethyl phosphite.[2] The possibility that **4-1** and **4-2** result from direct reaction of **1** with P($OMe)_3$ present as an impurity in the commercially obtained *t*-BuP($OMe)_2$ samples was eliminated by ^{1}H NMR analysis. Careful integration of the small δ 3.49 doublet corresponding to P($OMe)_3$ in a fresh sample of dimethyl *tert*-butylphosphonite against the ^{13}C satellite peaks of *t*-BuP(O*Me*$)_2$ established a phosphite impurity level of 0.21 mol %. Formation of **4-1** and **4-2** that were isolated in small but reproducible total yields of ca. 3% (based on *t*-BuP($OMe)_2$) by simple Arbuzov chemistry involving free P($OMe)_3$ present as an impurity can therefore be ruled out, and we conclude that the phosphonate products are the result of P—C bond cleavage.[30-32] Given the low isolated yields of **4-1** and **4-2**, one must also question whether trimethyl phosphite could be formed from dimethyl *tert*-butylphosphonite in the course of the reaction. Oxidation[33] and/or hydrolysis[33-36] of unreacted *t*-BuP($OMe)_2$ would produce the related phosphonic (*t*-BuP(O)($OMe)_2$) or phosphinic (*t*-BuP(O)H(OMe)) ester, respectively, with retention of the phosphorus–alkyl bond as the major product and, hence, is not a rational route to trimethyl phosphite and hence **4-1** and **4-2**. NMR experiments demonstrated that methylene chloride solutions of **3a-1** and **3a-2** were stable with respect to P—C bond cleavage at room temperature under preparative conditions and support our conclusion that the P—C bond cleavage products originate from the

(29) Aaron, H. S. *Topics in Stereochemistry*; Interscience: New York, 1979.

(30) Garrou, P. E. *Chem. Rev.* **1985**, *85*, 171–185.

(31) Doherty, N. M.; Hogarth, G.; Knox, S. A. R.; Macpherson, K. A.; Melchior, F.; Morton, D. A. V.; Orpen, A. G. *Inorg. Chim. Acta* **1992**, *198–200*, 257–270.

(32) Nakazawa, H.; Matsuoka, Y.; Nakagawa, I.; Miyoshi, K. *Organometallics* **1992**, *11*, 1385–1392.

(33) Corbridge, D. E. C. *Phosphorus: An Outline of Its Chemistry, Biochemistry and Technology*; Elsevier: Amsterdam, 1985.

(34) Daugherty, K. E.; Eychaner, W. A.; Stevens, J. I. *Appl. Spectrosc.* **1968**, *22*, 95–98.

(35) Sander, M. *Chem. Ber.* **1960**, *93*, 1220–1230.

(36) Sweigart, D. A. *J. Chem. Soc., Chem. Commun.* **1980**, 1159.

Table IV. Crystallographic Data

	3a-1	3a-2	3b-2
		Crystal Data	
formula	$CoC_{30}H_{37}INO_2P_2$	$CoC_{30}H_{37}INO_2P_2$	$CoC_{28}H_{33}INO_2P_2$
mol wt	691.4	691.4	663.36
cryst syst	orthorhombic	monoclinic	orthorthombic
space group	$P2_12_12_1$ (No. 19)	$P2_1$ (No. 4)	$P2_12_12_1$ (No. 19)
a, b, c (Å)	9.815(4), 14.314(6), 21.120(9)	13.073(5), 8.731(2), 13.537(5)	8.7004(7), 12.0769(18), 27.490(3)
α, β, γ (deg)	90, 90, 90	90, 106.49(3), 90	90, 90, 90
V (Å^3)	2967(2)	1481.5(9)	2888.5(6)
Z	4	2	4
cryst size (mm)	0.45 × 0.45 × 0.25	0.65 × 0.1 × 0.05	0.20 × 0.20 × 0.50
D_{calc} (g cm^{-3})	1.548	1.550	1.525
$F(000)$	1400	700	1335.83
		Data Collection	
temp (K)	198	198	299
radiation	Mo Kα (0.710 69 Å)	Mo Kα (0.710 69 Å)	Mo Kα (0.709 30 Å)
2θ range, deg	6.0–55.0	6.0–55.0	5.0–45.0
data collected (hkl)	0–12, −18 to +18, 0–27	−13 to +16, −8 to +11, −17 to +16	−2 to +8, −11 to +12, −29 to +29
abs cor	DIFABS[a] (0.75–1.27)	DIFABS[a] (0.90–1.12)	none
no. of reflns collected	7406	7079	5818
no. of unique rflns	6818	5743	3700
no. of reflns with $F \geq n\sigma(F)$	5958 (n = 4.0)	4846 (n = 4.0)	3118 (n = 2.5)
		Refinement	
no. of params	349	348	317
R, R_w	2.83, 2.99	3.19, 3.55	4.4, 4.9
GOF	1.15	1.02	0.68
η	1.02(3)	0.99(4)	1.39(14)
$(\Delta/\sigma)_{max}$	0.002	0.271	0.127
$\Delta(\rho)$ (max/min) (e Å^{-3})	+0.64/−0.71	+1.06/−0.56	+0.640/−0.850

[a] Empirical absorption corrections calculated using the program DIFABS.[48]

proposed cationic phosphonite intermediate **2**. We caution, however, that triethyl phosphite (ca. 7 mol %) has been detected in the AIBN-initiated autoxidation of ethyl diethylphosphonite under forcing conditions (323 K, p_{O_2} = 1.0 atm, $t_{1/2} = 10^3$ s).[37] ^{1}H NMR experiments showed that CD_2Cl_2 solutions of t-BuP(OMe)$_2$ are rapidly oxidized in air to give a complex mixture of products. Integration of the trimethyl phosphite δ 3.49 doublet against the total t-Bu signal showed ca. 0.5 mol % trimethyl phosphite; therefore, **2** remains as the primary source of **4-1** and **4-2** in the chemistry of Scheme I.

P—C bonds have approximately the same bond strength as C—C bonds (62 vs 64 kcal·mol^{-1}) and tend to resist cleavage unless activated. Although Knox and Orpen[31] have shown that electron-withdrawing phosphine substituents hinder P—C bond cleavage, the majority of reported low-oxidation-state examples can be constructively viewed as a cluster-mediated intramolecular oxidative addition[30] that produces a primary μ-phosphido product. P—C bond cleavage occurs with increasing difficulty as the s character of the P—C bond decreases (P—C_{sp} > P—C_{sp^2} > P—C_{sp^3}).[30] It appears unlikely then that the mechanism for the P—C bond cleavage of the Co(III) complexes proposed in this work parallels the oxidative-addition path found in the reaction of low-oxidation-state ([M]—PR_3)$_n$ derivatives[30,38] or the direct, base-catalyzed hydrolysis of P—C_{sp^3} reported for Pt(II) bis(diphenylphosphino)methane complexes under phase-transfer conditions.[39] An alternative path involving simple nucleophilic attack of iodide at C_α with cleavage of alkyl halide seems equally unlikely, especially for the bulky *tert*-butyl case.

Scheme II shows a proposed mechanism that involves

Scheme II

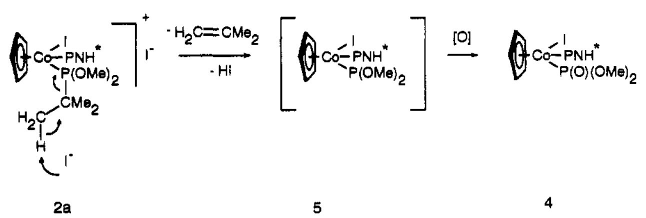

an iodide-assisted β-elimination of the initially formed cationic phosphonite complex[2] **2a**. This organometallic analog of classic phosphonium ion elimination would form an oxidatively unstable[40] phosphito intermediate and isobutylene. Subsequent oxidation affords the isolated products **4-1** and **4-2**.

P—C bond cleavage via β-elimination is not unprecedented. Goel[41] has reported the Pt(II)-promoted cleavage of P(t-Bu)$_3$ under very mild conditions. Pyrolysis of ethyl- and *tert*-butyl-substituted tertiary phosphine oxides[42] in the absence of catalysts produces ethylene and isobutylene but requires forcing conditions (ca. 773 K). Support for the elimination mechanism shown in Scheme II was obtained by ^{1}H NMR identification of isobutylene in the reaction of **1** and t-BuP(OMe)$_2$ in CD_2Cl_2. A CD_2Cl_2 sample containing a 1:1 mole ratio of **1** and t-BuP(OMe)$_2$ prepared in a sealed NMR tube showed multiplets at 4.66 and 1.73 ppm identical with those for an authentic sample of isobutylene.

Solid-State Structure, Chiroptical Properties, and Absolute Configuration. Suitable crystals of **3a-1**, **3a-2**, and **3b-2** were obtained by the slow cooling of toluene/hexane solutions at 243 K. Their solid-state structures were determined by X-ray diffraction techniques. Crystal

(37) Hwang, W.-S.; Yoke, J. T. *J. Org. Chem.* **1980**, *45*, 2088–2091.
(38) Ortiz, J. V.; Halvas, Z.; Hoffmann, R. *Helv. Chim. Acta* **1984**, *67*, 1–17.
(39) Lin, I. J. B.; Lai, J. S.; Liu, C. W. *Organometallics* **1990**, *9*, 530–531.
(40) Buhro, W. E.; Zwick, B. D.; Georgiou, S.; Hutchinson, J. P.; Gladysz, J. A. *J. Am. Chem. Soc.* **1988**, *110*, 2427–2439.
(41) Goel, A. B.; Goel, S. *Inorg. Chim. Acta* **1984**, *90*, L3–L34.
(42) Bailey, W. J.; Muir, W. M.; Marktsscheffel, F. *J. Org. Chem.* **1962**, *27*, 4404–4408.

Table V. Atomic Coordinates (×10[4]) and Isotropic Thermal Parameters (Å[2] × 10[4]) for 3a-1

atom	x	y	z	U(eq)[a]
Co	6854.7(4)	8363.7(3)	8376.4(2)	202(1)
I	9350.9(2)	7828.3(2)	8356.6(1)	322(1)
P(1)	6580.6(8)	7988.2(6)	7366.8(4)	200(2)
P(2)	6037.8(8)	6976.6(5)	8703.9(4)	211(2)
O(1)	4450(2)	7229(2)	8834(1)	293(6)
O(2)	6137(2)	6167(2)	8252(1)	277(7)
N	7071(3)	6922(2)	7155(1)	232(8)
C(1)	3351(4)	6600(3)	8695(2)	384(12)
C(2)	6617(3)	6502(2)	9495(1)	273(10)
C(3)	7956(4)	5982(3)	9413(2)	434(13)
C(4)	5540(5)	5813(3)	9713(2)	534(15)
C(5)	6815(5)	7251(3)	10003(2)	536(15)
C(6)	8147(3)	6681(2)	6702(2)	272(9)
C(7)	8767(5)	5748(3)	6901(2)	466(14)
C(11)	5742(4)	9006(2)	9104(2)	303(10)
C(12)	5202(3)	9230(2)	8500(2)	305(10)
C(13)	6227(4)	9743(2)	8170(2)	334(11)
C(14)	7395(4)	9786(2)	8549(2)	372(12)
C(15)	7097(4)	9322(2)	9133(2)	342(11)
C(21)	7397(3)	8762(2)	6792(2)	236(9)
C(22)	8496(3)	9335(2)	6947(2)	271(10)
C(23)	9134(3)	9879(2)	6497(2)	306(11)
C(24)	8686(4)	9852(3)	5875(2)	302(10)
C(25)	7592(4)	9298(2)	5708(2)	302(10)
C(26)	6946(3)	8762(2)	6160(2)	258(9)
C(31)	4777(3)	8063(2)	7151(1)	217(9)
C(32)	3989(3)	7263(3)	7185(2)	290(10)
C(33)	2586(3)	7306(3)	7085(2)	360(11)
C(34)	1971(4)	8150(3)	6956(2)	353(12)
C(35)	2755(4)	8957(3)	6909(2)	308(11)
C(36)	4155(3)	8907(2)	7005(2)	269(10)
C(41)	7610(4)	6625(2)	6025(2)	268(10)
C(42)	8466(4)	6821(3)	5520(2)	437(13)
C(43)	7946(5)	6766(3)	4896(2)	529(16)
C(44)	6603(6)	6527(3)	4792(2)	570(17)
C(45)	5783(5)	6332(3)	5286(2)	476(14)
C(46)	6272(4)	6370(3)	5908(2)	346(11)

[a] Equivalent isotropic U defined as one-third of the trace of the orthogonalized U_{ij} tensor.

Table VI. Atomic Coordinates (×10[4]) and Isotropic Thermal Parameters (Å[2] × 10[4]) for 3a-2

atom	x	y	z	U(eq)[a]
Co	2679.2(4)	5191.0(8)	3894.8(4)	197(2)
I	3282.9(2)	8000	4031.0(2)	286(1)
P(1)	3079(1)	4712(1)	2438(1)	189(3)
P(2)	1009(1)	5782(2)	3012(1)	229(4)
O(1)	388(3)	4175(5)	3066(3)	353(12)
O(2)	840(3)	6279(4)	1919(2)	291(11)
N	2899(3)	6185(5)	1630(3)	217(12)
C(1)	−297(5)	3440(8)	2176(5)	487(24)
C(2)	232(4)	7174(7)	3602(4)	320(18)
C(3)	298(6)	8751(8)	3161(5)	487(23)
C(4)	−942(5)	6650(9)	3263(5)	489(24)
C(5)	621(4)	7245(9)	4789(4)	424(21)
C(6)	3302(4)	6213(6)	714(3)	247(15)
C(7)	2531(4)	7166(8)	−125(4)	379(19)
C(11)	2112(4)	4085(7)	4993(4)	341(18)
C(12)	2510(3)	3012(9)	4411(3)	326(14)
C(13)	3626(4)	3296(6)	4615(3)	319(18)
C(14)	3899(4)	4566(7)	5263(4)	337(17)
C(15)	2944(4)	5067(8)	5496(3)	345(17)
C(21)	4484(3)	4240(6)	2622(3)	233(14)
C(22)	4819(3)	3080(8)	2084(3)	285(13)
C(23)	5893(3)	2881(9)	2172(4)	341(16)
C(24)	6642(4)	3839(7)	2792(4)	347(18)
C(25)	6320(4)	4995(7)	3339(4)	310(17)
C(26)	5261(3)	5195(6)	3253(3)	258(14)
C(31)	2353(3)	3067(9)	1710(3)	246(12)
C(32)	1591(3)	3337(6)	763(3)	287(18)
C(33)	998(4)	2146(7)	216(4)	339(17)
C(34)	1150(4)	671(7)	606(4)	382(19)
C(35)	1889(4)	379(7)	1540(4)	350(18)
C(36)	2498(5)	1599(6)	2084(4)	309(17)
C(41)	4425(4)	6866(6)	961(3)	258(15)
C(42)	5159(4)	6244(7)	507(4)	329(17)
C(43)	6189(5)	6853(8)	709(5)	457(22)
C(44)	6481(4)	8088(10)	1381(4)	467(19)
C(45)	5759(5)	8686(8)	1839(4)	467(21)
C(46)	4734(4)	8108(8)	1638(3)	339(15)

[a] Equivalent isotropic U defined as one-third of the trace of the orthogonalized U_{ij} tensor.

data and atomic coordinates are listed in Tables IV–IX. Pluto drawings of the solid-state molecular structures obtained are reproduced in Figures 1–3. In each case the coordination geometry about cobalt is pseudooctahedral, typical for three-legged piano-stool complexes, with unexceptional η^5-Cp, iodide, aminophosphine, and monodentate, distorted-pyramidal, P-bonded phosphinate ligands. Monodentate interligand bond angles approach 90° (∠P–Co–P (av) = 91.6(9)°, ∠P–Co–I(av) = 93.8(15)°) and the Cp–Co(av) (2.103(25) Å), Co–P(N)(av) (2.213(6) Å), and Co–P(O)(av) (2.231(18) Å) bond lengths are in the normal range for Co(III).

The absolute configurations of **3a-1**, **3a-2**, and **3b-2** were unequivocally assigned from their X-ray structures shown in Figures 1–3. The chirality parameter η[43] was refined to 1.02(3), 0.99(4), and 1.39(14) for **3a-1**, **3a-2**, and **3b-2**, respectively, showing that the stereochemistry was assigned the correct hand. The stereogenic carbon center derived from the chiral pool was known to be *S* in each case and provided an independent check for the correctness of the configurational assignments. Consideration of **3a-1**, **3a-2**, and **3b-2** as pseudotetrahedral cases with η^5-Cp occupying one coordination site and use of the modified Cahn–Ingold–Prelog rules[44,45] with the ligand priority series for Co I > η^5-Cp > P(O)(OMe)(R) > PPh$_2$NHC*H(Me)Ph specifies the absolute configurations of **3a-1**, **3a-2**, and **3b-2** as $S_{Co};R_P;S_C$, $R_{Co};S_P;S_C$, and $R_{Co};S_P;S_C$, respectively.

The absolute configurations of **3b-1**, **3b-3**, and **3b-4** were assigned on the basis of chiroptical data and Co epimerization cycles. Solution isomerization of $R_{Co};S_P;S_C$-**3b-3** by Co epimerization[2,26] gives exclusively **3b-2**; hence, the former can be assigned the absolute configuration $S_{Co};S_P;S_C$. Figure 4 shows that the CD spectra of the high- and low-R_f diastereomers **3a-1** and **3a-2** are quasi-mirror images, as expected for piano-stool transition-metal epimers.[2,19,26,28] The CD spectra of **3a-2** and **3b-2**, which were both established by X-ray data to be R_{Co}, show the same morphology as **3b-4**; thus, assuming that the absolute configuration of the transition metal dominates CD spectra,[28] **3b-4** must have the same absolute configuration at cobalt (R_{Co}). Further, since **3b-3** is established to be $S_{Co};S_P;S_C$ and is *not* Co epimeric with respect to **3b-4**, the latter must have the absolute configuration $R_{Co};R_P;S_C$. **3b-1** is then $S_{Co};R_P;S_C$, confirmed by solution epimerization to **3b-4** and by the morphology of its CD spectrum (cf. Figure 4).

Conformational Analysis. Examination of the crystal structures of **3a-1**, **3a-2**, and **3b-2** (Figures 1–3) shows that a "*chaise longue*" conformation, formed as the result of intramolecular P=O···H—N hydrogen bonding, is established in the solid state (cf. Chart I). The N—O distances 2.716, 2.829, and 2.648 Å determined for **3a-1**, **3a-2**, and **3b-2** respectively reflect strong O···H—N hydrogen bond-

(43) Rogers, D. *Acta. Crystallogr., Sect. A* **1981**, *37*, 734–741.
(44) Stanley, K.; Baird, M. C. *J. Am. Chem. Soc.* **1975**, *97*, 6598–6599.
(45) Sloan, T. E. *Top. Stereochem.* **1981**, *12*, 1–36.

Table VII. Atomic Coordinates and Isotropic Thermal Parameters (Å^2) for 3b-2

atom	x	y	z	B_{iso}^{a}
I	0.56964(12)	0.02944(10)	0.20116(4)	5.57(5)
Co	0.30317(24)	0.11878(18)	0.18836(6)	4.49(9)
P(1)	0.2408(4)	0.0118(3)	0.12621(12)	3.46(15)
P(2)	0.3964(5)	0.2485(3)	0.13971(14)	4.97(20)
O(1)	0.2481(17)	0.3310(10)	0.1321(5)	8.3(8)
O(2)	0.4619(11)	0.2159(7)	0.0917(3)	4.3(4)
N	0.3827(10)	−0.0060(8)	0.0867(3)	3.1(4)
C(1)	0.227(3)	0.3977(16)	0.0906(7)	8.2(11)
C(2)	0.535(4)	0.3401(18)	0.1679(7)	10.5(15)
C(3)	0.687(3)	0.358(3)	0.1464910)	12.9(18)
C(6)	0.3708(16)	−0.0741(10)	0.0426(4)	3.5(6)
C(7)	0.4640(18)	−0.0193(13)	0.0024(5)	5.3(7)
C(11)	0.209(3)	0.2459(18)	0.2318(7)	8.0(12)
C(12)	0.0900(23)	0.1861(17)	0.2071(7)	7.2(10)
C(13)	0.0983923)	0.0773(17)	0.2260(6)	6.6(10)
C(14)	0.221(3)	0.0664(19)	0.2565(6)	7.6(12)
C(15)	0.293(3)	0.1723(25)	0.2610(6)	8.5(13)
C(21)	0.1756(16)	−0.1307(12)	0.1422(5)	4.2(6)
C(22)	0.2379(18)	−0.1821(14)	0.1826(6)	6.0(8)
C(23)	0.2018(23)	−0.2889(15)	0.1960(9)	7.7(11)
C(24)	0.104(3)	−0.3463(15)	0.1651(7)	7.1(11)
C(25)	0.0385(23)	−0.2987(14)	0.1244(7)	6.6(9)
C(26)	0.0808(21)	−0.1905(13)	0.1127(5)	5.3(8)
C(31)	0.0753(18)	0.0654(10)	0.0923(4)	3.5(6)
C(32)	−0.0743(18)	0.0521(12)	0.1080(5)	4.8(7)
C(33)	−0.1919(17)	0.1049(15)	0.0827(6)	5.3(8)
C(34)	−0.1638(18)	0.1634(14)	0.0422(6)	5.2(8)
C(35)	−0.0174(18)	0.1774(13)	0.0260(5)	4.5(7)
C(36)	0.1033(15)	0.1289(12)	0.0500(5)	3.9(6)
C(41)	0.4328(18)	−0.1925(12)	0.0500(4)	4.1(7)
C(42)	0.5385(19)	−0.2161(13)	0.0855(6)	5.3(8)
C(43)	0.5980(20)	−0.3247(16)	0.0888(7)	7.0(10)
C(44)	0.549(3)	−0.4047(13)	0.0556(7)	7.0(11)
C(45)	0.447(3)	−0.3808(13)	0.0214(7)	6.9(11)
C(46)	0.3821(19)	−0.2753(13)	0.0178(6)	5.6(8)

^{a} B_{iso} is the mean of the principal axes of the thermal ellipsoid.

Table VIII. Selected Bond Lengths (Å) for 3a-1, 3a-2, and 3b-2

bond	3a-1	3a-2	3b-2
Co–I	2.567(1)	2.567(1)	2.581(2)
Co–P(1)	2.215(1)	2.218(2)	2.209(4)
Co–P(2)	2.250(1)	2.213(1)	2.213(5)
Co–C(11)	2.098(3)	2.078(6)	2.112(18)
Co–C(12)	2.058(4)	2.060(8)	2.090(18)
Co–C(13)	2.114(4)	2.129(5)	2.120(17)
Co–C(14)	2.136(4)	2.144(5)	2.102(17)
Co–C(15)	2.119(4)	2.098(5)	2.100(15)
P(1)–N	1.661(3)	1.661(4)	1.659(9)
P(1)–C(21)	1.829(3)	1.829(5)	1.865(14)
P(1)–C(31)	1.831(3)	1.845(6)	1.833(15)
P(2)–O(1)	1.623(2)	1.633(4)	1.644(13)
P(2)–O(2)	1.504(2)	1.497(4)	1.490(9)
P(2)–C(2)	1.892(3)	1.900(6)	1.808(22)
O(1)–C(1)	1.435(4)	1.432(7)	1.408(23)
N–C(6)	1.467(4)	1.480(7)	1.469(15)

ing[46,47] typical for the basic phosphoryl P=O group. Their solid-state conformations are remarkably similar to that found for other hydrogen-bonded aminophosphine phosphonate, phosphinate,[2,3,19,26] and acyl[47] analogs in which intramolecular noncovalent interactions dominate stereoelectronic preferences. The η^5-Cp group occupies a pseudoequatorial and the iodide a pseudoaxial position in the Co—P—N—H···O=P six-membered ring. An alternate conformation in which iodide is pseudoequatorial appears much less favorable since, as a consequence of the pseudooctahedral geometry at the metal and concomitant

(46) Whuler, A.; Brouty, C.; Spinat, P. *Acta Crystallogr.* **1980**, *B36*, 1267–1269.

(47) Korp, J. D.; Bernal, I. *J. Organomet. Chem.* **1981**, *220*, 355–364.

Table IX. Selected Bond Angles (deg) for 3a-1, 3a-2, and 3b-2

angle	3a-1	3a-2	3b-2
I–Co–P(1)	91.6(1)	95.7((1)	94.7(1)
I–Co–P(2)	94.7(1)	93.0(1)	92.8(1)
P(1)–Co–P(2)	92.2(1)	90.5(1)	92.1(1)
Co–P(1)–N	116.5(1)	114.4(2)	113.6(4)
Co–P(1)–C(21)	116.0(1)	113.7(2)	115.6(5)
N–P(1)–C(21)	104.5(1)	102.3(2)	105.1(5)
Co–P(1)–C(31)	110.1(1)	114.0(2)	112.4(4)
N–P(1)–C(31)	105.5(1)	107.2(2)	105.1(5)
C(21)–P(1)–C(31)	102.9(1)	104.0(2)	101.9(6)
Co–P(2)–O(1)	101.4(1)	101.6(1)	102.6(5)
Co–P(2)–O(2)	117.5(1)	116.3(1)	119.2(4)
O(1)–P(2)–O(2)	109.9(1)	110.9(2)	110.3(6)
Co–P(2)–C(2)	118.8(1)	118.8(1)	114.7(8)
O(1)–P(2)–C(2)	102.7(1)	101.5(2)	101.9(10)
O(2)–P(2)–C(2)	105.3(1)	106.5(2)	106.6(10)
P(1)–N–C(6)	126.9(2)	123.1(3)	124.2(8)

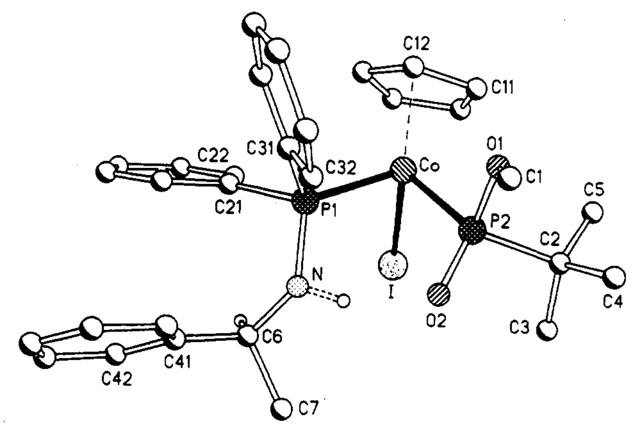

Figure 1. Molecular structure of **3a-1**.

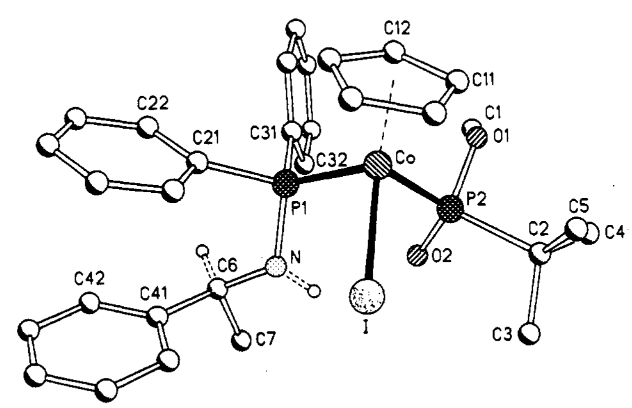

Figure 2. Molecular structure of **3a-2**.

90° interligand bond angles, it almost eclipses the pseudoaxial phosphorus substituents (cf. Chart II). In agreement with the proposed axial orientation of iodide the solid-state I-Co-P-O and I-Co-P-C torsional angles are in the range 158–173° (cf. Cart II).

^{1}H nuclear Overhauser effect difference spectroscopy (NOED)[2,3,19,26] established that the solid-state "*chaise longue*" conformation of **3** is retained in solution. The NOED experiments shown in Figure 5 show that partial saturation of the Cp resonance in **3a-1** gives positive NOE enhancements for the *ortho* hydrogens of the diastereotopic aminophosphine $P(C_6H_5)_2$ (7.5%, 9.7%), the $P(t\text{-}C_4H_9)$ (1.4%), and the $POCH_3$ (1%) substituents. Reference to Chart II shows that both phenyl groups of the aminophosphine as well as both phosphinate substituents are *gauche* and therefore proximal to the η^5-Cp ring *provided that η^5-Cp is pseudoequatorial.* Similar NOED results were obtained for the remaining diastereomers in

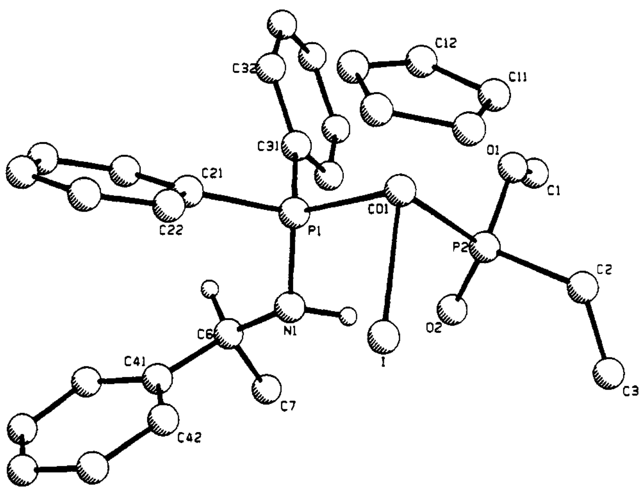

Figure 3. Molecular structure of **3b-2**.

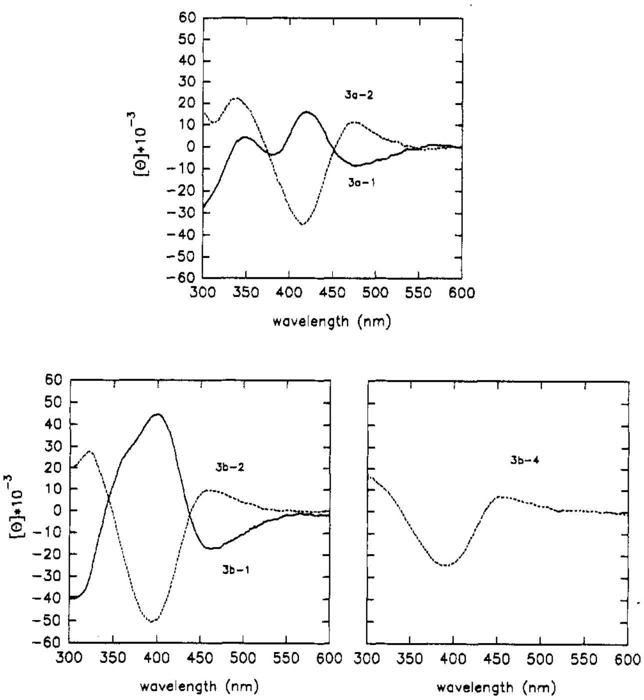

Figure 4. Circular dichroism spectra: (top) **3a-1** (solid line) and **3a-2** (dotted line); (bottom left) **3b-1** (solid line) and **3b-2** (dotted line); (bottom right) **3b-4**.

the series **3a** and **3b**. In this conformation the $S_{Co};R_P;S_C/R_{Co};S_P;S_C$ diastereomers **3a-1**/**3a-2** or **3b-1**/**3b-2** place the phosphinate alkyl substituent, R, in a pseudoequatorial position (Chart I, left side). In contrast, the $R_{Co};R_P;S_C/S_{Co};S_P;S_C$ diastereomers **3b-3**/**3b-4** force R to occupy a pseudoaxial position (Chart I, right side) which may be of little consequence for R = ethyl but very unfavorable for R = *tert*-butyl.

Optical Yields and Reaction Mechanism. Assumption of the product-like transition state for the dealkylation of prochiral phosphonite **2** → **3** (cf. Scheme I and Chart I) implies that 1,3-diaxial steric interactions of the P(N) and P(O) substituents of the hydrogen-bonded "*chaise longue*" template control the product stereochemistry. Chart I predicts that the $S_{Co};R_P$ or $R_{Co};S_P$ diastereomer with less severe 1,3-diaxial interactions will be the major product. In the case of the *tert*-butyl series where *tert*-butyl/phenyl vs methoxy/phenyl 1,3-diaxial interactions result in a maximum energy difference for the diaste-

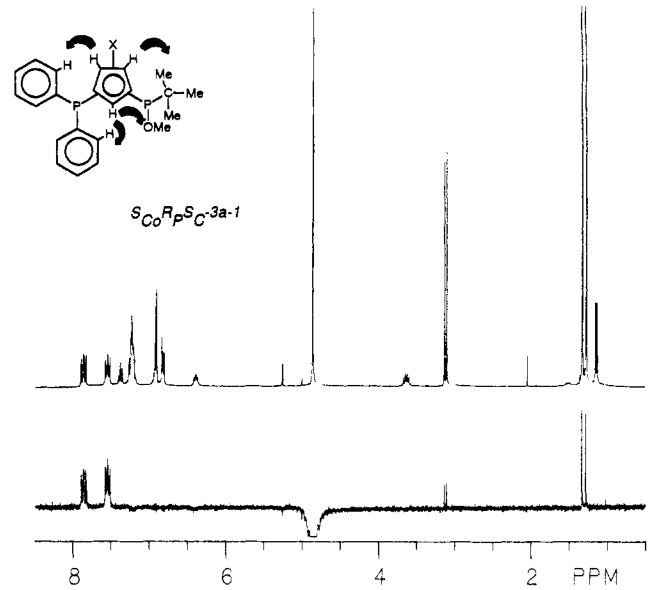

Figure 5. ^{1}H NOED spectra of **3a-1**: (top) reference (X 1/64); (bottom) difference spectrum with Cp resonance irradiated.

Chart II

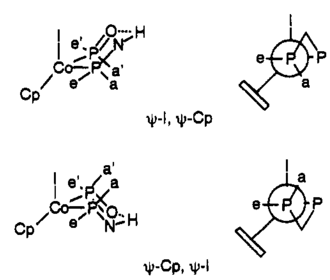

	dihedral angles (deg) (I-Co-P-a), (I-Co-P-a')
3a-1	169.7, 171.4
3a-2	158.0, 167.5
3b-2	167.6, 172.5

reotopic transition states, the NMR-determined kinetic product distribution showed the optical yield to be 100%. No $S_{Co};S_P$ or $R_{Co};R_P$ diastereomers were observed. Since the chirality at carbon is identical in both cases, there is no chirality transfer from the aminophosphine. Optical induction originates exclusively from the chiral cobalt atom.

The case for the ethyl phosphinate products is less clear since the energy difference for ethyl/phenyl versus methoxy/phenyl 1,3-diaxial interactions is diminished, and it can be expected that optical yields will be degraded. Nevertheless, as found for the *tert*-butyl analogs, the absolute configuration of the major products obtained is correctly predicted with the prior assumption that P(O)—R steric requirements are greater than P(O)—OMe steric requirements. If S_{Co} forms on initial substitution of diastereotopic iodide in **1** (ca. 50% probability), the kinetic product is $S_{Co};R_P;S_C$ (≤25% de based on isolated product). Formation of R_{Co} results in $R_{Co};S_P;S_C$ (≤14% de based on isolated product). These low optical yields presumably reflect the limited steric differentiation between –OMe and $-CH_2Me$ in the transition state and support the proposal that 1,3-diaxial interactions are the essential component in the chiral induction step. When these steric interactions are diminished, chiral induction falls. Optical yields for the R = ethyl series **3b** obtained from product isolation studies should be treated with caution; nevertheless, comparison of the results reported in this study with earlier work[2] shows that Co→P optical induction decreases with decreasing steric requirement of the phosphonite substituent, $RP(OMe)_2$, along the series R = t-C_4H_9 > C_6H_5 > C_2H_5 (cf. Table I).

Conclusion

Prochiral dimethyl *tert*-butyl- and ethylphosphonite complexes prepared *in situ* by halide substitution of (η^5-Cp)CoI_2($PPh_2NHC^*H(Me)Ph$) undergo diastereoselective Arbuzov-like dealkylation to produce P-chiral phosphinate products. Optical induction originates from the chiral cobalt atom and is transmitted to phosphorus primarily via steric interactions on a conformationally restricted "*chaise longue*" template. Increasing steric demands of the phosphonite substituent increase 1,3-steric interactions in the transition state for dealkylation and lead to improved optical yields. Products resulting from P—C bond cleavage form in low yield from the reaction of 1 with dimethyl *tert*-butylphosphonite and dimethyl ethylphosphonite. Isobutylene formation in the reaction of 1 with dimethyl *tert*-butylphosphonite strongly supports a mechanism involving β-elimination.

Experimental Section

Reagents and Methods. All manipulations were performed under a nitrogen atmosphere in a MBraun glovebox or using standard Schlenk techniques. Nitrogen gas was purified by passing through a series of columns containing DEOX (Alfa) catalyst heated to 393 K, granular phosphorus pentoxide, and activated 3A molecular sieves. Toluene, benzene, and hexane were distilled from blue solutions of sodium benzophenone ketyl. Methylene chloride was freshly distilled from P_4O_{10}. Acetone and ethyl acetate were distilled from activated 3A molecular sieves. NMR spectra were recorded on a General Electric 300-NB Fourier transform spectrometer operating at a proton frequency of 300.12 MHz. Infrared spectra were measured on a Mattson Polaris Fourier transform spectrometer as a solution in 0.1-mm-pathlength KBr cells or as a thin film on a KBr disk. Optical rotation measurements were determined in toluene (ca. 1 mg/mL) in a 1-cm-pathlength cell using a Perkin-Elmer Model 141 polarimeter. Circular dichroism spectra were determined in toluene (ca. 1 mg/mL) on a Jasco J40 A apparatus using a 0.1-cm-pathlength cell. Melting points were determined in sealed capillaries and are uncorrected. Elemental analyses were performed by Guelph Chemical Laboratories Inc., Guelph, Ontario, Canada, or Canadian Microanalytical Services, Inc., Delta, BC, Canada. Chromatographic purifications were carried out using a Chromatotron (Harrison Associates) with 1–4 mm thick silica $gel_{60}PF_{254}$ (Merck) adsorbent.

The compound (η^5-Cp)CoI_2((*S*)-(–)-$PPh_2NHC^*H(Me)$-Ph)[2] was prepared using the literature procedure. Commercial samples of dimethyl *tert*-butylphosphonite (Organometallics or Alfa), dimethyl ethylphosphonite (Organometallics), and isobutylene (Aldrich) were used as received.

Proton nuclear Overhauser enhancement difference (NOED) spectra were determined under steady-state conditions[48] on a GE 300-NB instrument using a set of 16K interleaved experiments of 16 or 32 transients cycled 12–16 times through the list of decoupling frequencies. The temperature was thermostated at 298.0 ± 0.1 K. In each experiment the decoupler was gated on in continuous wave (CW) mode for 4–6 s with sufficient attenuation to give an approximate 70–90% reduction in intensity of the irradiated peak. A 60-s delay preceded each frequency change. A set of four "dummy" scans was employed to equilibrate the spins prior to data acquisition. No relaxation delay was applied between successive scans at a given decoupling frequency. Difference spectra were obtained on 16K or zero-filled 32K data tables which had been digitally filtered with a 1–2-Hz exponential line-broadening function.

Crystal Structure Determination of 3a-1 and 3a-2. Data were collected on a Stoe-Siemens R3m/V four-circle diffractometer (Braunschweig) at 198 K in profile mode using graphite-monochromated Mo Kα radiation. The structures were solved by the heavy-atom method and refined anisotropically on F, minimizing the function $\sum w(F_o - F_c)^2$, where $w^{-1} = \sigma^2(F) + 0.0002F^2$ for **3a-1** and $w^{-1} = \sigma^2(F) + 0.0003F^2$ for **3a-2**. Hydrogen atoms were included in the refinement by using a riding model. Absolute configurations were determined by Rogers' η method.[43] In each case the stereochemical assignments were confirmed by comparison of the absolute configuration at carbon, which was known to be *S*. The program system was SHELXTL PLUS (written by Prof. G. M. Sheldrick), which incorporates scattering factors from ref 49.

Crystal Structure Determination of 3b-2. Data were collected at room temperature on an Enraf-Nonius CAD 4 automated diffractometer (Ottawa) under the control of the NRCCAD program[50] using graphite-monochromated Mo Kα radiation. Trial structures were obtained by direct methods, with further structure refinements via successive cycles of least-squares and difference Fourier calculations using the NRCVAX suite of structure-solving programs.[51] Hydrogens were placed at the calculated positions. The absolute configuration was determined by Rogers' η method.[43] The stereochemical assignment was confirmed by comparison of the absolute configuration at carbon, which was known to be *S*.

Reaction of (η^5-Cp)CoI_2($PPh_2NHC^*H(Me)Ph$) with t-BuP(OMe)$_2$. Preparation of (R,S_{Co};R,S_P;S_C)-(η^5-Cp)CoI($PPh_2NHC^*H(Me)Ph$)(P(O)(OMe)(t-Bu)) (3a) and (R,S_{Co})-(η^5-Cp)CoI($PPh_2NHC^*H(Me)Ph$)(P(O)-(OMe)$_2$) (4). A solution of 0.2147 g (1.430 mmol) of t-BuP-(OMe)$_2$ in 10 mL of methylene chloride was added dropwise over 15 min to a stirred solution of 0.9793 g (1.461 mmol) of 1 in 40 mL of the same solvent in a glovebox (N_2). The deep purple solution became orange and then slowly turned brown-green. Stirring was continued for an additional 1.5 h; then the crude, brown-green reaction mixture was removed from the glovebox and filtered. Removal of volatiles under aspirator pressure left a black residue which

(48) Neuhaus, D.; Williamson, M. P. *The Nuclear Overhauser Effect in Structural and Conformational Analysis*; VCH: New York, 1989.
(49) *International Tables for X-Ray Crystallography*; Kynoch Press: Birmingham, U.K., 1975.
(50) NRCCAD-An Enhanced CAD4 Control Program. Presented at the American Crystallography Association Annual Meeting, 1986; p 24.
(51) Gabe, E. J.; LePage, Y.; Charland, J. P.; Lee, F. L.; White, P. S. *J. Appl. Crystallogr.* **1989**, *22*, 384–387.
(52) Walker, N.; Stuart, D. *Acta Crystallogr., Sect. B* **1983**, *A39*, 158–166.

was purified without protection from air by radial thick-layer chromatography on 2-mm silica gel plates. Elution with 3:1 benzene/ethyl acetate separated, in order of decreasing R_f values, purple starting material 1 (0.4767 g, 48.68%) followed by brown zones which contained **3a-1** and **3a-2** (0.1213 g, 24.20% and 0.1265 g, 25.17%, respectively, based on recovered 1), and yellow-brown zones containing 4-1 and 4-2 (12.6 mg, 2.58% and 13.3 mg, 2.72%, respectively, based on recovered 1). Recrystallization of **3a-1** and **3a-2** by slow cooling of hexane/toluene solutions of the chromatographically separated material at 243 K gave essentially diastereomerically pure products.

Reaction of (η^5-Cp)CoI$_2$(PPh$_2$NHC*H(Me)Ph) with EtP(OMe)$_2$. Preparation of (R,S_{Co};R,S_P;S_C)-(η^5-Cp)-CoI(PPh$_2$NHC*H(Me)Ph)(P(O)(OMe)(Et)) (3b). A solution of 0.816 g (6.68 mmol) of EtP(OMe)$_2$ in 20 mL of methylene chloride was slowly added to a stirred solution of 4.60 g (6.86 mmol) of 1 in 50 mL of the same solvent. Heating the reaction mixture in a sealed Carius tube at 333 K overnight resulted in a color change from deep purple to yellow brown. Removal of volatiles at 0.1 Torr left a dark, sticky solid which was taken up in a small volume of 2:1 benzene/ethyl acetate and chromatographed through a short silica gel column with 1:1 benzene/ethyl acetate and then acetone as eluent. The initial yellow zone was discarded, and the remaining yellow crude product mixture was collected and then rechromatographed on a preparative radial 4 mm silica gel plate. A series of yellow fractions were collected using benzene/ethyl acetate (2:1) as eluent. Compounds **3b-1** (291 mg, 7.27%) and **3b-2** (401 mg, 9.95%) eluted first and were separated; however, it was not possible to obtain pure samples of the remaining diastereomers. Continued elution with 2:1 benzene/ethyl acetate gave fractions rich in **3b-3** (176 mg, 4.37%) and **3b-4** (303 mg, 7.52%). ^{1}H NMR analysis showed traces of the P—C bond cleavage products **4-1** and **4-2**. Diastereomer **3b-2** was crystallized from toluene/hexane at 243 K.

Epimerization of (S_{Co};R_P;S_C)- and (S_{Co};R_P;S_C)-(η^5-Cp)CoI(P(O)(OMe)Et)(PPh$_2$NHC*H(Me)Ph) (3b-1 and 3b-2). Samples of **3b-1** and **3b-2**, isolated chromatographically, were dissolved in boiling cyclohexane and then cooled to room temperature. After it stood overnight, TLC analysis showed the solution to be enriched in diastereomers **3b-4** and **3b-3**, respectively. No other diastereomers were detected.

Acknowledgment. This work was supported by a Natural Sciences and Engineering Council of Canada (NSERC) Operating Grant (C.R.J.) and a summer research fellowship (B.J.B.). P.G.J. acknowledges the financial support provided by the Fonds der Chemischen Industrie (Frankfurt/Main, Germany). We are indebted to Dr. E. Gabe, Chemistry Division, NRC, Ottawa, Canada, for X-ray facilities and assistance in determining the crystal structure of **3b-2**.

Supplementary Material Available: Tables giving structure determination summaries for **3a-1** and **3a-2** and tables of additional bond lengths and angles, anisotropic thermal parameters for non-H atoms, and positional parameters for H atoms for **3a-1**, **3a-2**, and **3b-2** (20 pages). Ordering information is given on any current masthead page.

OM930158A